Research Article

Jin-Hae Chang*

Equibiaxially stretchable colorless and transparent polyimides for flexible display substrates

https://doi.org/10.1515/rams-2020-0003
Received Sep 27, 2019; accepted Dec 11, 2019

Abstract: 4,4′-(4,4′-isopropylidenediphenoxy)bis(phthalic anhydride) (BPADA) was reacted with three structurally different diamines to produce poly(amic acid)s, which were then imidized to produce colorless and transparent polyimide (CPI) films through stepwise thermal cyclization. The three amines used to synthesize CPI based on BPADA are: bis(3-aminophenyl)sulfone (APS), *p*-xylyenediamine (*p*-XDA), and bis[4-(3-aminophenoxy)-phenyl] sulfone (*m*-BAPS). The obtained CPI films were almost colorless and exhibited excellent optical transparencies. The solubility of the CPI films in various solvents was investigated, and all the CPI films were found to be soluble in common solvents such as chloroform, dichloromethane, *N,N*'-dimethyl acetamide, and pyridine. The thermo-optical properties and oxygen transmission rates (O_2TRs) of the CPI films were examined for various biaxial stretching ratios in the range of 100–150%, and their properties were compared. When the stretching ratio changed from 100 to 150%, the glass transition temperature and yellow index did not show any significant change; however, the O_2TR decreased for all CPI films.

Keywords: colorless and transparent polyimide; organosoluble polyimide; equibiaxial stretching; thermo-optical property; gas permeation

1 Introduction

Recently, various techniques have been developed to synthesize colorless and transparent polyimides (CPIs). For example, a -CF_3 group, which is a strong electron-withdrawing group, is often used as a substituent, or bent monomer structures are used to prevent charge-transfer complexes (CT complexes) from being formed in linear structures [1–3]. The resulting CPIs exhibit superior solubility, gas-barrier property, and optical properties, compared to other commercialized PIs [4–6]. CPIs with such outstanding characteristics find applications in several fields, as flexible electronic polymeric materials [5, 6].

CPIs can replace the glass in display devices, and have many applications in electronic devices. They can provide great advantages when used in electronic devices because they can be synthesized easily and mass-produced. Optically, CPI films are great alternatives for the glasses that are widely in flat-panel displays such as plasma discharge panels (PDPs) and liquid crystal displays (LCDs) [7, 8]. Over the past few years, the use of flexible and transparent materials with a conducting oxide layer such as indium tin oxide (ITO) has increased in the fields of display substrates and microelectronics [8-10]. However, ITOs have some drawbacks because indium is a rare and expensive element, which requires processing at high temperatures to achieve good purity when applied on to glass plates. Moreover, glass cannot be used as a display material because it is fragile and not flexible [8]. Therefore, CPI is one of the best alternative materials to overcome the drawbacks of glass.

In the meantime, many researchers have used 4,4′-(4,4′-isopropylidenediphenoxy) bis(phthalic anhydride) (BPADA) anhydride for PI synthesis [11–13]. BPADA has a bended structure as a whole and does not have a -CF_3 substituent on its structure. Thus, if PI is synthesized using BPADA monomer, PI shows colorless and transparent characteristics. Some groups [12, 13] used BPADA to synthesize new PIs, and others [14, 15] used BPADA monomers to make nanocomposites. In particular, our group [16] and Huang *et al.* [15] used BPADA to synthesize PI nanocomposites using functionalized graphenes. However, studies on CPI films using biaxial stretching have not yet been published.

Many works have reported the effects of uni- or biaxial-orientation on the morphology and crystalline behaviors of polymer films [17, 18]. Biaxial stretching means stretching in one direction and stretching perpendicularly to that direction, or stretching it in both directions at the same

***Corresponding Author: Jin-Hae Chang:** Department of Polymer Science and Engineering, Kumoh National Institute of Technology, Gumi 39177, Korea; Email: changjinhae@hanmail.net

time. Stretching makes the polymer structure of the film directional, increases the gas barrier, and improves the tensile strength and modulus. These methods are also commonly used in the film industry to improve the physical properties and introduce birefringence in films.

Many engineering polymer films such as poly(ethylene terephthalate) (PET), poly(lactic acid) (PLA), and polyamide (PA) are used in biaxial stretching processes. Most of these films are used for packaging food and snacks such as chips, breads, biscuits, etc.; they are also used as electronic encapsulating materials [19, 20]. However, in most cases, stretching of the PI film has been reported to cause whitening and/or damage to the film. The whitening phenomenon ultimately leads to deterioration of the optical transparency and physical properties of the PI film [21, 22]. Studies on stretching of the PI films have been quite rare. However, if the monomer structures in PIs are designed well, the PI films can be stretched without any whitening, regardless of the transparency.

The gas permeabilities are closely related to the sizes of the side groups and substituents and the chemical structure of the main chain. For example, bulky side groups or substituents disrupt molecular packing in the polymer chains, thereby increasing the free volume, which in turn, decreases the barrier property [23, 24]. The stretching of the film also has a great effect on the gas barrier property. The gas molecules transmitted through the polymer film are affected by the degree to which they are oriented by the stretching of the film. In fact, chemical structural packing resulting from stretching reduces the diffusion coefficient of the gases passing through the polymer film. This reduction in diffusion coefficient is due to the dense molecular packing caused by the stretching of the molecular structure [23–26].

In this work, we synthesized CPI films through the thermal cyclization of a precursor CPI obtained by the reaction of 4,4′-(4,4′-isopropylidenediphenoxy)bis(phthalic anhydride) (BPADA) with three different diamine monomers: bis(3-aminophenyl) sulfone (APS), *p*-xylyenediamine (*p*-XDA), and bis[4-(3-aminophenoxy) phenyl] sulfone (*m*-BAPS). To clarify the relationship between the structure and properties of the CPI films, this paper explains the properties of the CPIs synthesized from the dianhydride BPADA and three different aromatic diamines, as mentioned previously.

This paper also describes the thermal properties, optical transparency, solubility, and oxygen permeability of the CPI films, as functions of the different diamine monomers. We also examine and compare the effects of varying the equibiaxial stretching ratio in the range 100–150% on the thermal properties, optical transparency, and oxygen permeability of the CPI films.

2 Experimental

2.1 Materials

The dianhydride and diamine monomers were purchased from Aldrich Chemical Co. (Yongin, Korea) and TCI (Tokyo, Japan), and were used without purification. *N,N′*-dimethylacetamide (DMAc) was purified and stored in molecular sieves (4 Å).

2.2 Preparation of CPI films

Three different CPIs (designated as samples I–III) were synthesized from BPADA and three diamines, namely, APS (sample I), *p*-XDA (sample II), and *m*-BAPS (sample III). The chemical structures of the synthetic route are shown in Figure 1.

As the synthesis methods of the three CPI films are almost the same, we will describe the synthesis process of BPADA/APS (sample I) only, representatively. Poly(amic acid) (PAA) was synthesized by reacting BPADA and APS dissolved in DMAc. BPADA (6.8 g; 1.3×10^{-2} mol) and DMAc (40 mL) were placed in a beaker and reacted at 0°C for 30 min under nitrogen atmosphere. 20 mL of DMAc was added to another beaker with APS solution, and was mixed

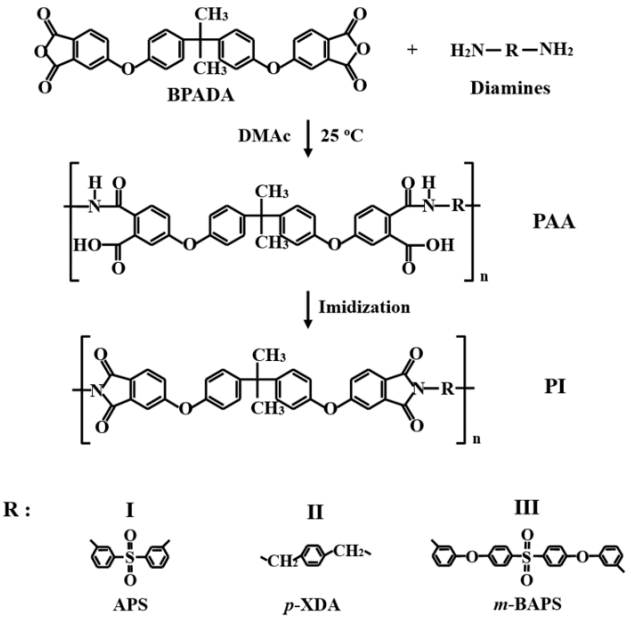

Figure 1: Synthetic routes for CPIs based on BPADA.

Table 1: Synthetic conditions of CPI films based on BPADA.

Sample	Temperature (°C) / time (hr) / pressure (Torr)
PAA	0/1/760 → 25/14/760 → 50/2/760 → 80/1/1
CPI	110/0.5/760 → 140/0.5/760 → 170/0.5/760 → 200/0.5/760 → 230/0.5/760 → 250/0.5/760

Table 2: Thermal properties of CPIs based on BPADA.

Monomer	I.V.[a]	T_g(°C)	T_D^{ib}(°C)	wt_R^{600c}(%)	CTE[d] (ppm/°C)
I	0.87	204	503	57	43.94
II	0.94	182	509	34	58.02
III	0.92	196	527	59	52.43

[a] Inherent viscosities were measured at 0.1 g/dL concentration in *N,N′*-dimethylacetamide at 30°C.

[b] 2% initial decomposition temperature.

[c] Weight % of the residue at 600°C.

[d] Coefficient of thermal expansion range was 50–150 °C.

with the already prepared BPADA solution. The solution was stirred strongly at 0°C for one hour and at 25°C for 14 h. The obtained PAA solution was poured onto a flat glass plate and the solvent was removed at 50°C over two hours to obtain a film. The CPI film was obtained through stepwise heating under various temperature conditions. Table 1 shows the heat treatment conditions for the synthesis of the CPI film, in detail. The inherent viscosities of the CPIs were between 0.87 and 0.94 at a concentration of 0.1 g/dL at 30 (C, as shown in Table 2.

2.3 Biaxial stretching of CPI film

The films were equibiaxially stretched using a biaxial stretching machine, with stretching ratios in the range 100–150% at a strain rate of 1 mm/s. The stretching temperatures were 260°C for APS (sample I), 240°C for p-XDA (sample II), and 255°C for m-BAPS (sample III). The obtained films were warped and torn into wave patterns when the stretching temperatures exceeded the optimum temperature.

The biaxial stretching of all CPI films proceeded in the same manner. No whitening was observed even when the biaxial stretching ratio was 150%. When all the CPI films were stretched biaxially by more than 150%, the surface became nonuniform and tore, failing to produce a good film.

2.4 Characterization

Differential scanning calorimetry (DSC) and thermogravimetric analysis (TGA) were performed under N_2 conditions using the DuPont 910 equipment. The samples were heated and cooled at a rate of 20°C/min. The coefficients of thermal expansion (CTEs) of the films were evaluated with a macro-expansion probe (TMA-2940), which was used to apply an expansion force of 0.1 N to the films at a heating rate of 5°C/min in the temperature range of 50–150°C.

The ultraviolet-visible (UV-vis) spectra of the CPI films were recorded on a Shimadzu UV-3600 instrument. The color intensity of the CPI film was measured using a Minolta spectrophotometer. The film was usually 71–76 µm thick. A CIE-D light source was used, and the CIELAB color difference equation was used to obtain the value of yellow index (YI). The O_2 permeability of the sample was obtained by the ASTM E-96 method using Mocon DL 100. The O_2 transmission rate (O_2TR) was measured at a temperature of 23°C, relative humidity of 0%, and pressure of 760 Torr. The CPI film was stretched biaxially, with a 4 × 4 stretching magnification, using a biaxial stretching tester (X6H-S, Toyo Seiki-Sho Ltd).

3 Results and discussion

3.1 FT-IR analysis

The formation of PAA and the completion of imide formation from amic acid were confirmed by examining FT-IR spectra; the spectra of PAA and the PIs are shown in Figure 2. Only representative IR results for sample I (BPADA/APS) is discussed here. The C=O stretching peaks

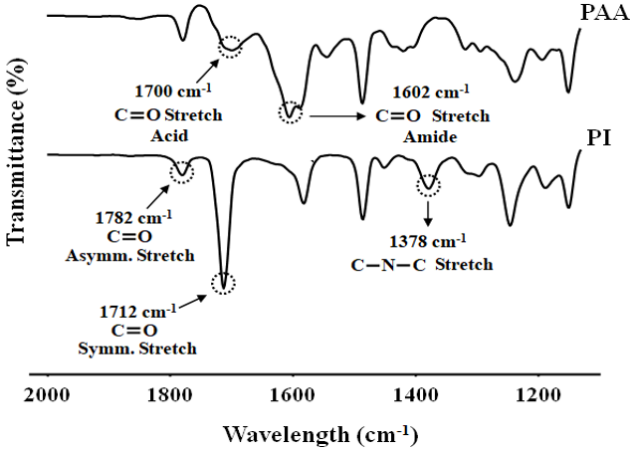

Figure 2: FT-IR spectra of PAA and PI (sample I).

at 1700 and 1602 cm^{-1} are due to the acid and amide groups of PAA, and shift to higher frequencies in the imides, specifically to approx. 1782 cm^{-1} (C=O, in phase) and 1712 cm^{-1} (C=O, out of phase). In addition, the presence of a feature at 1378 cm^{-1} corresponding to C-N-C stretching confirms the formation of the imides [27].

3.2 Thermal behavior

The thermal behaviors of the CPIs fabricated using three different diamines are listed in Table 2. The glass transition temperatures (T_g) were in the range of 182–204°C, depending on the structure of the diamine. The molecular chains containing the sulfonyl (SO_2) group (APS, sample I) were much stiffer and rigid than those containing methylene (*p*-XDA, sample II) or ether (*m*-BAPS, sample III) linkages. Thus, the T_g value for sample I (204°C) was higher than that of the CPIs containing *p*-XDA (182°C) or *m*-BAPS (196°C) (see Table 2). The factors affecting the increase in T_g value were: (1) the effects of the rigid rod-like monomer structures on the free volume of the polymer, and (2) the restriction of inter-reacting polymer chains within the polymers, which prevented the segmental motion of the chains [28, 29]. The DSC curves of the CPIs with the three different diamine monomers are shown in Figure 3.

The initial decomposition temperatures (T_D^i) of samples I–III were in the range of 503–527°C (see Table 2). In sample I, because of the difficulty in rotating freely about its own axis, the rigid SO_2 group caused high torsional deformation. In addition, SO_2 could be released easily because of the steric hindrance and conformational energy produced by the high torsion under high temperatures. As a result, SO_2 separated easily into radicals [30]. Hence, the CPI containing SO_2 groups showed the lowest T_D^i value. The T_D^i of sample II was lower than that of sample III because of the presence of flexible alkyl ($-CH_2-$) linkages, which degraded easily upon heating. However, sample III exhibited a higher T_D^i than sample I because of the presence of a larger number of phenyl groups and the flexible ether linkage between the phthalimide units. These ether linkages allowed the free rotation of the SO_2 group, inhibiting the dissociation of SO_2 radicals in *m*-BAPS. The wt_R^{600} of samples I–III were in the range of 34–59%. Sample III exhibited a higher wt_R^{600} (59%) than sample I (57%) because of the presence of a larger number of phenyl groups per monomer unit in the entire molecular structure. Sample II showed the lowest weight residue (34%) because of the low thermal stability of the alkyl structure in the main chain. The TGA thermograms of samples I–III are shown in Figure 4.

The CTE depends on molecular rearrangement. High molecular rearrangement produces low CTE values and, eventually, low residual stress. When the temperature increases, the in-plane–oriented CPI molecules tend to relax in a direction normal to their original direction and, eventually, expand mainly in the out-of-plane direction [31, 32]. In the case of samples I–III, the rigid rod-type molecular structure present in the main chain made the movement of molecules difficult, and this led to low CTE values. The CTE values of the CPIs were 43.94–58.02 ppm/°C, depending on the molecular structure, and the values are summarized in Table 2. Sample I showed the lowest value of 43.94 ppm/°C because it was easy to build up close molecular packing because of the rigid rod-type SO_2 structure and high intermolecular attraction between the molecular chains and chains, resulting in lower CTE [33, 34]. On the other hand, sample II showed the highest CTE of 58.02 ppm/°C because of the flexible ($-CH_2-$) linkages, which reduced the close packing. The CTE results obtained for various stretching ratios are shown in Figure 5.

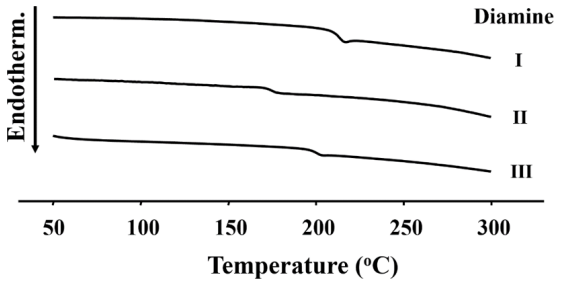

Figure 3: Differential scanning calorimetry (DSC) thermograms of CPIs based on BPADA.

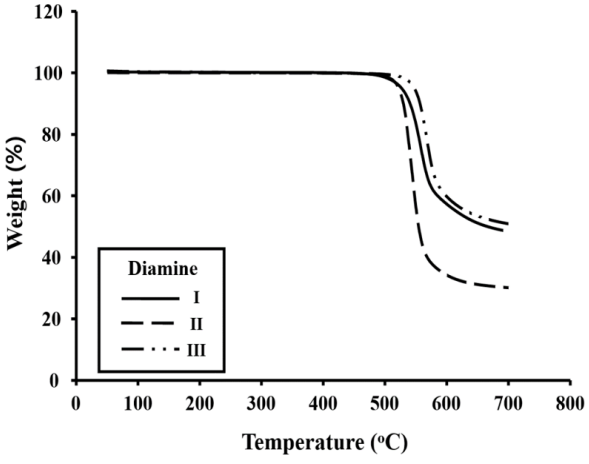

Figure 4: Thermogravimetric analysis (TGA) thermograms of CPIs based on BPADA.

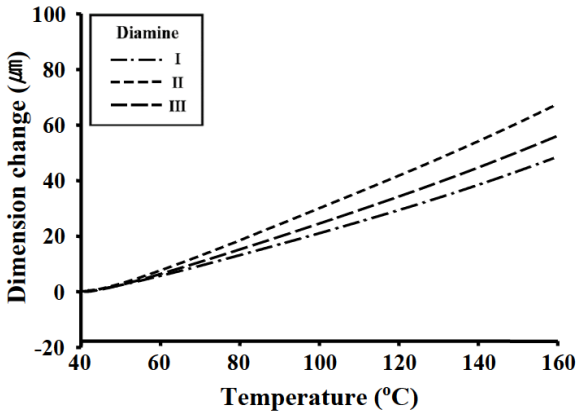

Figure 5: TMA thermograms of CPIs based on BPADA.

3.3 Optical transparency

The optical properties of all solvent-cast CPI films were measured using a UV-vis. spectrometer, and the results are shown in Figure 6. The optical transparencies of the CPIs were clarified from the cutoff wavelengths (λ_o), transmittance at 550 nm, and yellow index (YI), as listed in Table 3. λ_o is the first wavelength at which the transmittance occurs. YI is an index value indicating the degree of yellow.

Table 3: Optical properties of CPIs based on BPADA.

Monomer	Film thickness (μm)	λ_0^a (nm))	550 nm^{trans} (%)	YI[b]
I	76	371	98	1.27
II	73	362	92	2.15
III	71	358	92	2.62

[a] Cutoff wavelength. [b] Yellow index.

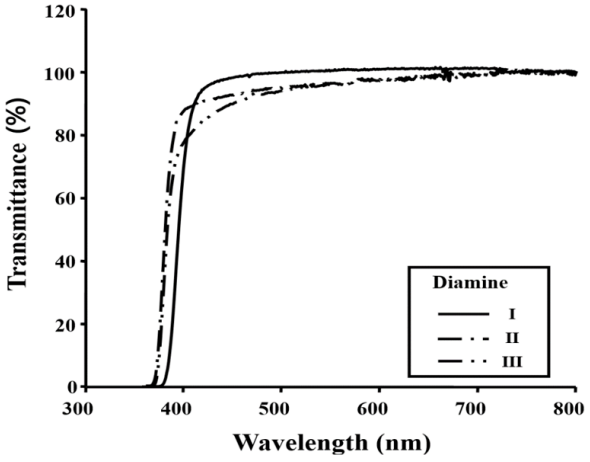

Figure 6: Ultraviolet-visible (UV-vis) transmittances of CPIs based on BPADA.

All CPI films showed values of λ_o < 400 nm and 92–98% transmittance at 550 nm. CPI films containing SO_2 (sample I) showed the lowest YI value (YI = 1.27), and sample I was almost colorless. In general, it can be said that it is colorless when the YI value is 5 or less. The value of YI was almost similar to that of poly(methyl methacrylate) (PMMA) (YI ≈ 1.50) [35].

Sample I, which contained SO_2, showed lower YI values than samples II and III with methylene and ether linkages, respectively. The electron-withdrawing and bulky SO_2 group in the diamine monomer probably contributed to the decrease of CT complexes between the main chains through steric hindrance and inductive effects [36]. On the contrary, the electron-donating ether group (Sample III) increased the intermolecular CT complexes by supplying electrons to the main chain phthalimide moiety, resulting in a higher YI value (YI = 2.62), as shown in Table 3. However, all CPI films containing different diamine monomers were almost colorless and transparent; the letters could be read easily through the films (see Figure 7). The transparency of the sample I was observed with varying stretching ratios of 100% to 150% in order to maintain transparency even after biaxial stretching, as shown in Figure 8. Regardless of the biaxial stretching %, all films were clear and transparent and no whitening was observed.

The colorlessness and transparency of the CPI films based on BPADA could be described by the reduction of intermolecular interaction. The bent structure and ether linkages in BPADA were effective in interrupting the CT complex formation between the polymer chains through steric hindrance and inductive effect [36, 37].

Figure 7: Photographs of CPI films based on BPADA.

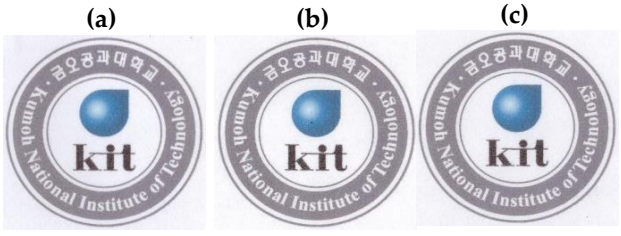

Figure 8: Photographs of sample I films for various equibiaxial stretching ratios. (a) 100 % (unstretched), (b) 130 %, and (c) 150 %.

Table 4: Solubility of CPIs based on BPADA.

Monomer	Acetone	$CHCl_3$	CH_2Cl_2	DMAc	DMF	DMSO	CH_3OH	NMP	Pyridine	THF	Toluene
I	×	◎	◎	◎	O	×	×	◎	◎	O	×
II	×	◎	◎	◎	×	×	×	◎	◎	◎	×
III	×	◎	◎	◎	O	×	×	O	◎	△	×

◎: Excellent, O: Good, △: Poor, ×: Very poor.

DMAc: *N,N'*-dimethylacetamide, DMF: *N,N'*-dimethylformamide, DMSO: dimethyl sulfoxide, NMP: *N'*-methyl-2-pyrrolidone, THF: tetrahydrofuran.

Table 5: Thermo-optical properties of CPIs based on BPADA for various equibiaxial stretching ratios.

Biaxial stretching ratio (%)	I		II		III	
	T_g (°C)	YI [a]	T_g (°C)	YI	T_g (°C)	YI
100 (unstretched)	204	1.27	182	2.15	196	2.62
120	207	1.31	184	1.86	196	2.60
130	206	1.20	184	1.97	197	2.89
150	205	1.28	184	2.23	196	2.28

[a] Yellow index.

3.4 Solubility

CPI is a very special polymer material that is very strong and has heat and chemical resistance [38, 39]. However, because of the fully cyclized structure, it is often not melted or dissolved, which limits its use as an engineering material. Hence, solubility will influence its processability for polymeric applications [40, 41].

The solubilities of the CPIs were measured in various solvents and the results are summarized in Table 4. Samples I–III exhibited somewhat limited solubility. All the films were soluble in chloroform, dichloromethane, *N,N'*-dimethyl acetamide (DMAc), and pyridine; however, they were insoluble in acetone, dimethyl sulfoxide (DMSO), methanol, and toluene.

The solubility of sample II was better than that of samples I and III in NMP and THF. The difference in solubility depends on the monomer structure present in the main chain. Sample II with a flexible methylene structure had weak molecular chain interactions and could not provide effective close packing, resulting in increased solubility [1, 36, 42]. However, the solubility level was not affected significantly by the CPI composition in terms of the molecular structure of the diamine.

3.5 Thermo-optical properties of equibiaxially stretched films

In general, polymer films such as polyethylene (PE), polypropylene (PP), poly (vinyl chloride) (PVC), and poly (ethylene terephthalate) (PET), which are used as packaging materials, are uniaxial- and biaxial-stretched. However, most polymer films used in electronic- and flexible display-materials are used after biaxial stretching in consideration of optical properties [18, 20, 22].

Table 5 lists the T_g and YI of the unstretched CPIs and the CPIs with various equibiaxial stretching ratios. Compared to the unstretched CPIs, the T_g of the CPIs with various biaxial stretching ratios appeared to be virtually unchanged, regardless of the stretching ratio varying from 120 to 150%. As a result, biaxial stretching has little effect on free volume or segmental motion, and thus does not significantly affect T_g.

The YI values obtained for various stretching ratios are also summarized in Table 5. Even though the stretching ratio increased from 120% to 150%, the YI values of all samples were almost constant and all the films were colorless and transparent. In addition, there was no difference when compared with the unstretched film (100%). From these results, it was found that stretching ratios had no effect on the clarity and optical properties of the CPI films. The transparencies of the films stretched to various percentages are not shown here because they are the same as the results in Table 5.

3.6 Oxygen permeability of the equibiaxially stretched films

There are two important factors necessary to obtain a polymer film with increased gas barrier properties [43, 44]: (1)

Table 6: Oxygen permeabilities of CPIs based on BPADA for various equibiaxial stretching ratios.

Biaxial stretching ratio (%)	I		II		III	
	O_2TR [a]	P_{st}/P_p [b]	O_2TR	P_{st}/P_p [b]	O_2TR	P_{st}/P_p [b]
100 (unstretched)	0.64	1	2.03	1	3.62	1
120	0.53	0.83	1.04	0.51	0.05	0.01
130	0.43	0.67	0.34	0.17	0.07	0.02
150	0.37	0.58	0.37	0.18	0.06	0.02

[a] Oxygen transmission rate (cc/m^2/day). [b] Stretched polymer permeability/unstretched polymer permeability (*i.e.*, relative permeability rate).

the main chains in the polymer must be stiffened by hindering intra-rotational movements, and (2) the intermolecular close packing of the main chains can suppress good permeability.

In this work, our results are explained in terms of the relative permeability P_{st}/P_p, where P_p is the permeability of the unstretched polymer and P_{st} is the permeability of the stretched polymer. The O_2TR of CPI films with various equibiaxial stretching ratios ranging from 100 to 150% are summarized in Table 6. Compared to samples II and III, the molecular chains containing SO_2 groups in sample I were straighter and harder than those containing methylene and ether linkages; thus, the O_2TR of sample I (0.64 cc/m^2/day) could be expected to be lower than that of sample II (2.03 cc/m^2/day) or sample III (3.62 cc/m^2/day).

For equibiaxial stretching ratios between 100 and 130%, the O_2TR of sample I was found to decrease linearly from 0.64 to 0.43 cc/m^2/day (33% reduction). When the stretching ratio increased up to 150%, the O_2TR decreased to 0.37 cc/m^2/day. This tendency could be attributed to the orientation of the CPI film molecules by stretching, which showed a greater effect on gas barrier properties as the stretching ratio increased [45–47].

The O_2TRs for samples II and III with various equibiaxial stretching ratios were measured, and are summarized in Table 6. The O_2TR of sample II decreased from 2.03 to 0.34 cc/m^2/day (83% reduction) as the biaxial stretching ratio increased to 130%, and then remained constant for stretching ratios up to 150% (0.37 cc/m^2/day). Similar behavior was observed in the case of sample III. The O_2TR of sample III decreased significantly when the biaxial stretching ratio changed from 100 to 120%, and then leveled off upon stretching to more than 120%. For example, the biaxial stretching of only 120% for sample III resulted in 99% reduction of O_2TR (0.05 cc/m^2/day), with respect to that of the unstretched PI film (3.62 cc/m^2/day). As the biaxial stretching ratio changed from 120 to 150%, the O_2TR of sample III remained fairly constant (0.05–0.07 cc/m^2/day) and close to zero. This reduction in O_2TR is closely related not only to diffusion by changes in polymer chains during biaxial stretching but also to solubility between film and gas. The permeation is explained by the following equation [47]

$$P = D \times S$$

Where, P = permeation, D = diffusion, and S = solubility.

The D value can be explained by the movement of the polymer chains changed by biaxial stretching. As the crystallization of the polymer chain increases with the increase of the biaxial stretching ratio, the P value decreases. However, the S value obtained between film and gas is very difficult to explain. Since our sample showed no change in thermal and optical properties even if the stretching ratio increased from 100 to 150%, our results can be assumed to be affected more by S than the D effect.

4 Conclusions

The T_g of CPI films containing three different amine monomers were in the range of 182–204°C, and thermal degradation was not observed at temperatures below 500°C, indicating excellent thermal stability. The CTE values of the three CPI films were in the range of 43.94–58.02 ppm/°C. Optical transparencies showed 92–98% transmittance at 550 nm and the YI values were in the range of 1.27–2.62; *i.e.*, almost colorless. The O_2TR values were slightly different, depending on the amine structure, but they were usually in the range of 0.64–3.62 cc/m^2/day.

The CPI films were equibiaxially stretched with stretching ratios ranging from 120 to 150%, and the T_g and O_2TR of the stretched films were investigated in detail. The T_g of the films appeared virtually unchanged in the DSC thermograms, regardless of the biaxial stretching ratios up to 150%. The values of O_2TR, however, decreased upon increasing the stretching ratio.

In conclusion, it appears that the structure of the diamine monomers influences the thermal properties, optical transparency, solubility, and gas permeation of the CPI films. We strongly claim that the present CPI films are vi-

able candidates for flexible display substrates in electro-optical applications even though their long-term reliability needs to be tested further.

Acknowledgement: This research was supported by the Basic Science Research Program of the National Research Foundation of Korea (NRF), funded by the Ministry of Education (2018R1D1A1B07045502).

References

[1] Maya, E. M., A. E. Lozano, J. Abajo, and J. G. Campa. Chemical modification of copolyimides with bulky pendent groups: Effect of modification on solubility and thermal stability. *Polymer Degradation & Stability*, Vol. 92, No. 12, 2007, pp. 2294–2299.

[2] Savard, O., T. J. Peckham, Y. Yang, and S. Holdcroft. Structure–property relationships for a series of polyimide copolymers with sulfonated pendant groups. *Polymer*, Vol. 49, No. 23, 2008, pp. 4949–4959.

[3] Kim, S.-U., C. Lee, S. Sundar, W. Jang, S.-J. Yang, and H. Han. J. Synthesis and characterization of soluble polyimides containing trifluoromethyl groups in their backbone. Polym. Sci., Part B. *Polym. Phys.*, Vol. 42, 2004, pp. 4303–4312.

[4] Liaw, D.-J., B.-Y. Liaw, and C.-W. Yu. Synthesis and characterization of new organosoluble polyimides based on flexible diamine. *Polymer*, Vol. 42, No. 12, 2001, pp. 5175–5179.

[5] Wang, L., Z. Zhao, J. Li, and C. Chen. Synthesis and characterization of fluorinated polyimides for pervaporation of n-heptane/thiophene mixtures. *European Polymer Journal*, Vol. 42, No. 6, 2006, pp. 1266–1272.

[6] Tian, Y., S. Liu, H. Ding, L. Wang, B. Liu, and Y. Shi. Formation of deformed honeycomb-patterned films from fluorinated polyimide. *Polymer*, Vol. 48, No. 8, 2007, pp. 2338–2344.

[7] Wang, P.-C., and A. G. MacDiarmid. Integration of polymer-dispersed liquid crystal composites with conducting polymer thin films toward the fabrication of flexible display devices. *Displays*, Vol. 28, No. 3, 2007, pp. 101–104.

[8] Choi, M.-C., Y. Kim, and C.-S. Ha. Polymers for flexible displays: From material selection to device applications. *Progress in Polymer Science*, Vol. 33, No. 6, 2008, pp. 581–630.

[9] Burrows, P. E., G. L. Graft, M. E. Gross, P. M. Martin, M. K. Shi, M. Hall, E. Mast, C. Bonham, W. Bennett, and M. B. Sullivan. Ultra barrier flexible substrates for flat panel displays. *Displays*, Vol. 22, No. 2, 2001, pp. 65–69.

[10] Chiang, C.-J., C. Winscom, S. Bull, and A. Monkman. Mechanical modeling of flexible OLED devices. *Organic Electronics*, Vol. 10, No. 7, 2009, pp. 1268–1274.

[11] Choi, I. W., and J.-H. Chang. Characterization of Colorless and Transparent Polyimide Films Synthesized with Various Amine Monomers. *Polymer (Korea)*, Vol. 35, No. 5, 2010, pp. 480–484.

[12] Chen, B.-K., Y.-T. Fang, and J.-R. Cheng. Synthesis of Low Dielectric Constant Polyetherimide Films. *Macromolecular Symposia*, Vol. 242, No. 1, 2006, pp. 34–39.

[13] Eichstadt, A. E., T. C. Ward, M. D. Bagwell, D. L. Farr, and J. E. McGrath. Synthesis and Characterization of Amorphous Partially Aliphatic Polyimide Copolymers Based on Bisphenol-A Dianhydride. *Macromolecules*, Vol. 35, No. 20, 2002, pp. 7561–7568.

[14] Yoonessi, M., D. A. Scheiman, M. Dittler, J. A. Peck, J. Ilavsky, J. R. Gaier, and M. A. Meador. High-temperature multifunctional magnetoactive nickel graphene polyimide nanocomposites. *Polymer*, Vol. 54, No. 11, 2013, pp. 2776–2784.

[15] Huang, T., R. Lu, C. Su, H. Wang, Z. Guo, P. Liu, Z. Huang, H. Chen, and T. Li. Chemically modified graphene/polyimide composite films based on utilization of covalent bonding and oriented distribution. *ACS Applied Materials & Interfaces*, Vol. 4, No. 5, May 2012, pp. 2699–2708.

[16] Heo, C., and J.-H. Chang. Polyimide nanocomposites based on functionalized graphene sheets: Morphologies, thermal properties, and electrical and thermal conductivities. *Solid State Sciences*, Vol. 24, 2013, pp. 6–14.

[17] Prattipati, V., Y. S. Hu, M. S. Bandi, D. A. Schiraldi, A. Hiltner, and E. Baer. Improving the transparency of stretched poly(ethylene terephthalate)/polyamide blends. *Journal of Applied Polymer Science*, Vol. 99, No. 1, 2006, pp. 225–235.

[18] Rajeev, R. S., E. Harkin-Jones, K. Soon, T. McNally, G. Menary, C. G. Armstrong, and P. J. Martin. Studies on the effect of equibiaxial stretching on the exfoliation of nanoclays in polyethylene terephthalate. *European Polymer Journal*, Vol. 45, No. 2, 2009, pp. 332–340.

[19] Masuda, J., and M. Ohkura. Preparation and characterization of biaxially oriented polypropylene film with high molecular orientation in the machine direction by sequential biaxial stretching. *Journal of Applied Polymer Science*, Vol. 106, No. 6, 2007, pp. 4031–4037.

[20] Hu, Y. S., V. Prattipati, A. Hiltner, E. Baer, and S. Mehta. Improving transparency of stretched PET/MXD6 blends by modifying PET with isophthalate. *Polymer*, Vol. 46, No. 14, 2005, pp. 5202–5210.

[21] Choi C.-H., Y.-M. Kim, and J.-H. Chang. Colorless and transparent polyimide films for flexible displays. *Polymer Science and Technology*. Vol. 23, 2012, pp. 296-306.

[22] King, J.-S., W. T. Whang, W.-C. Lee, and L.-M. Chang. Effect of backbone on the biaxial retardation of polyimide films in uniaxial stretch. *Materials Chemistry and Physics*, Vol. 103, No. 1, 2007, pp. 35–40.

[23] Jang, J., and D. K. Lee. Oxygen barrier properties of biaxially oriented polypropylene/polyvinyl alcohol blend films. *Polymer*, Vol. 45, No. 5, 2004, pp. 1599–1607.

[24] Fan, B. G., L. D. Maio, L. Incarnato, P. Scarfato, and D. Acierno. The relative significance of biaxial stretch ratio effects on the permeability of oriented PET film. *Packaging Technology & Science*, Vol. 13, No. 3, 2000, pp. 123–132.

[25] Terui, Y., and S. Ando. J. Coefficients of molecular packing and intrinsic birefringence of aromatic polyimides estimated using refractive indices and molecular polarizabilities. Polym. Sci., Part B. *Polym. Phys.*, Vol. 42, 2004, pp. 2354–2366.

[26] Perrin-Sarazin, F., M. Ton-That, M. Bureau, and J. Denault. Micro- and nano-structure in polypropylene/clay nanocomposites. *Polymer*, Vol. 46, No. 25, 2005, pp. 11624–11634.

[27] Pavia, D. L., G. M. Lampman, and G. S. Kriz. *Introduction to spectroscopy*. Chapt 2. Harcourt Brace College Publishers, New York, 2008, Chapter 2, pp. 14–95.

[28] Fernandez-Blazquez, J. P., and A. Bello. E, Perez. Observation of Two Glass Transitions in a Thermotropic Liquid-Crystalline Polymer. *Macromolecules*, Vol. 37, 2004, pp. 9018–9026.

[29] Ash, B. J., L. S. Schadler, and R. W. Siegel. Glass transition behavior of alumina/polymethylmethacrylate nanocomposites. *Mate-*

rials Letters, Vol. 55, No. 1-2, 2002, pp. 83–87.

[30] Butt, M. S., Z. Akhtar, M. Z. Zaman, and A. Munir. Synthesis and characterization of some novel aromatic polyimides. *European Polymer Journal*, Vol. 41, No. 7, 2005, pp. 1638–1646.

[31] Min, U., J. C. Kim, and J.-H. Chang. Transparent polyimide nanocomposite films: Thermo-optical properties, morphology, and gas permeability. *Polymer Engineering and Science*, Vol. 51, No. 11, 2011, pp. 2143–2150.

[32] Tyan, H. L., Y. C. Liu, and K. H. Wei. Thermally and Mechanically Enhanced Clay/Polyimide Nanocomposite via Reactive Organoclay. *Chemistry of Materials*, Vol. 11, No. 7, 1999, pp. 1942–1947.

[33] Numata, S., S. Oohara, K. Fujisaki, J. Imaizumi, and N. Kinjo. Thermal expansion behavior of various aromatic polyimides. *Journal of Applied Polymer Science*, Vol. 31, No. 1, 1986, pp. 101–110.

[34] Liou, H.-C., P. S. Ho, and R. Stierman. Thickness dependence of the anisotropy in thermal expansion of PMDA-ODA and BPDA-PDA thin films. *Thin Solid Films*, Vol. 339, No. 1-2, 1999, pp. 68–73.

[35] Yang, C. P., and Y. Y. Su. Colorless and high organosoluble polyimides from 2,5-bis(3,4-dicarboxyphenoxy)-t-butylbenzene dianhydride and aromatic bis(ether amine)s bearing pendent trifluoromethyl groups. *Polymer*, Vol. 46, No. 15, 2005, pp. 5778–5788.

[36] Choi, I. H., and J.-H. Chang. Colorless polyimide nanocomposite films containing hexafluoroisopropylidene group. *Polymers for Advanced Technologies*, Vol. 22, No. 5, 2011, pp. 682–689.

[37] Yang, C. P., S. H. Hsiao, and Y. C. Chen. Soluble and light-colored polyimides from 2,3,2′,3′-oxydiphthalic anhydride and aromatic diamines. *Journal of Applied Polymer Science*, Vol. 97, No. 3, 2005, pp. 1352–1360.

[38] Chung, C. L., and S. H. Hsiao. Novel organosoluble fluorinated polyimides derived from 1,6-bis(4-amino-2-trifluoromethylphenoxy)naphthalene and aromatic dianhydrides. *Polymer*, Vol. 49, No. 10, 2008, pp. 2479–2485.

[39] Chen, K., X. C. Kazuaki, Y. N. Endo, M. Higa, and K. Okamoto. Synthesis and properties of novel sulfonated polyimides bearing sulfophenyl pendant groups for fuel cell application. *Polymer*, Vol. 50, No. 2, 2009, pp. 510–518.

[40] Ghaemy, M., R. Porazizollahy, and M. Bazzar. Novel thermal stable organosoluble polyamides and polyimides based on quinoxalin bulky pendent group. *Macromolecular Research*, Vol. 19, No. 6, 2011, pp. 528–536.

[41] Kim, M. H., M. H. Hoang, D. H. Choi, M. J. Cho, H. K. Ju, D. W. Kim, and C. J. Lee. Electro-optic effect of a soluble nonlinear optical polyimide containing two different chromophores with different sizes in the side chain. *Macromolecular Research*, Vol. 19, No. 4, 2011, pp. 403–407.

[42] Yang, C.-P., R.-S. Chen, and K.-H. Chen. Organosoluble and light-colored fluorinated polyimides based on 2,2-bis[4-(4-amino-2-trifluoromethylphenoxy)phenyl]propane and aromatic dianhydrides. *Journal of Applied Polymer Science*, Vol. 95, No. 4, 2005, pp. 922–935.

[43] Jarus, D., A. Hiltner, and E. Baer. Barrier properties of polypropylene/polyamide blends produced by microlayer coextrusion. *Polymer*, Vol. 43, No. 8, 2002, pp. 2401–2408.

[44] LeBaron, P. C., Z. W. Wang, and T. J. Pinnavaia. Polymer-layered silicate nanocomposites: An overview. *Applied Clay Science*, Vol. 15, No. 1-2, 1999, pp. 11–29.

[45] Kim, J. H., W. J. Koros, and D. R. Paul. Physical aging of thin 6FDA-based polyimide membranes containing carboxyl acid groups. Part I. Transport properties. *Polymer*, Vol. 47, No. 9, 2006, pp. 3094–3103.

[46] Liu, R. Y. F., Y. S. Hu, M. R. Hibbs, D. M. Collard, D. A. Schiraldi, A. Hiltner, and E. Baer. Improving oxygen barrier properties of poly(ethylene terephthalate) by incorporating isophthalate. I. Effect of orientation. *Journal of Applied Polymer Science*, Vol. 98, No. 4, 2005, pp. 1615–1628.

[47] Min, U., and J.-H. Chang. *Thick films: Properties, technology and applications* (I. P. Panzini, ed.). Nova Sci. Publisher Inc, New York, 2012, Chapter 5, pp. 261–282.